
Nonconvex Federated Learning on Compact Smooth Submanifolds With Heterogeneous Data

Jiaojiao Zhang

KTH Royal Institute of Technology
jiaoz@kth.se

Jiang Hu*

UC Berkeley
hujiangopt@gmail.com

Anthony Man-Cho So

The Chinese University of Hong Kong
manchoso@se.cuhk.edu.hk

Mikael Johansson

KTH Royal Institute of Technology
mikaelj@kth.se

Abstract

Many machine learning tasks, such as principal component analysis and low-rank matrix completion, give rise to manifold optimization problems. Although there is a large body of work studying the design and analysis of algorithms for manifold optimization in the centralized setting, there are currently very few works addressing the federated setting. In this paper, we consider nonconvex federated learning over a compact smooth submanifold in the setting of heterogeneous client data. We propose an algorithm that leverages stochastic Riemannian gradients and a manifold projection operator to improve computational efficiency, uses local updates to improve communication efficiency, and avoids client drift. Theoretically, we show that our proposed algorithm converges sub-linearly to a neighborhood of a first-order optimal solution by using a novel analysis that jointly exploits the manifold structure and properties of the loss functions. Numerical experiments demonstrate that our algorithm has significantly smaller computational and communication overhead than existing methods.

1 Introduction

Federated learning (FL), which enables clients to collaboratively train models without exchanging their raw data, has gained significant traction in machine learning [1, 2]. The framework is appreciated for its capacity to leverage distributed data, accelerate the training process via parallel computation, and bolster privacy protection. The majority of existing FL algorithms address problems that are either unconstrained or have convex constraints. However, for applications such as principal component analysis (PCA) and matrix completion, where model parameters are subject to nonconvex manifold constraints, there are very few options in the federated setting.

In this paper, we study FL problems over manifolds in the form of

$$\underset{x \in \mathcal{M} \subset \mathbb{R}^{d \times k}}{\text{minimize}} \quad f(x) := \frac{1}{n} \sum_{i=1}^n f_i(x), \quad f_i(x) = \frac{1}{m_i} \sum_{l=1}^{m_i} f_{il}(x; \mathcal{D}_{il}). \quad (1)$$

Here, n is the number of clients, x is the matrix of model parameters, and \mathcal{M} is a compact smooth submanifold embedded in $\mathbb{R}^{d \times k}$. For example, PCA-related optimization problems use the Stiefel manifold $\mathcal{M} = \text{St}(d, k) = \{x \in \mathbb{R}^{d \times k} : x^T x = I_k\}$ to maintain orthogonality [3, 4]. In (1), the global loss $f : \mathbb{R}^{d \times k} \rightarrow \mathbb{R}$ is smooth but nonconvex, and the local loss function f_i of each client i is the average of the losses f_{il} on the m_i data points in its local dataset $\mathcal{D}_i = \{\mathcal{D}_{i1}, \dots, \mathcal{D}_{im_i}\}$. In this

*Corresponding author

paper, we consider a heterogeneous data scenario where the statistical properties of \mathcal{D}_i differ across clients.

Manifold optimization problems of the form (1) appear in many important machine learning tasks, such as PCA [5, 6], low-rank matrix completion [7, 8], multitask learning [9, 10], and deep neural network training [11, 12]. Still, there are very few federated algorithms for machine learning on manifolds. In fact, the work [13] appears to be the only FL algorithm that can deal with manifold optimization problems of a similar generality as ours. Handling manifold constraints in an FL setting poses significant challenges: **(i)** Existing single-machine methods for manifold optimization [3, 14, 15] cannot be directly adapted to the federated setting. Due to the distributed framework, the server has to average the clients local models. Even if each of these models lies on the manifold, their average typically does not due to the nonconvexity of \mathcal{M} . The current literature relies on complicated geometric operators, such as the exponential map, inverse exponential map, and parallel transport, to design an averaging operator for the manifold [13]. However, these mappings may not admit closed-form expressions and can be computationally expensive to evaluate. For example, to evaluate the inverse exponential map on the Stiefel manifold one needs to solve a nonlinear matrix equation, which is computationally challenging [16]. **(ii)** Extending typical FL algorithms to scenarios with manifold constraints is not straightforward, either. Most existing FL algorithms either are unconstrained [17, 18] or only allow for convex constraints [19, 20, 21, 22, 23], but manifold constraints are typically nonconvex. Moreover, compared to nonconvex optimization in Euclidean space, manifold optimization necessitates the consideration of the geometric structure of the manifold and properties of the loss functions, which poses challenges for algorithm design and analysis. **(iii)** Traditional methods for enhancing communication efficiency in FL, like local updates [24], need substantial modifications to accommodate manifold constraints. The so-called client drift issue due to local updates and heterogeneous data [18] persists in the realm of manifold optimization. Directly using client-drift correcting techniques originally developed for Euclidean spaces [18, 25, 26] could lead to additional communication or computational costs due to the manifold constraints. For instance, in [13], the correction term requires additional communication of local Riemannian gradients and involves using parallel transport to move the correction term onto some tangent space in preparation for the exponential mapping. Although some existing decentralized manifold optimization algorithms [6, 27, 28] can be simplified to an FL scenario with only one local update under the assumption of a fully connected network, these algorithms cannot be directly applied to FL scenarios with more than one local update, especially in cases of data heterogeneity. Extending the analysis of these algorithms to FL scenarios with multiple local updates is not straightforward. On the other hand, the use of local updates in FL, compared to these decentralized distributed algorithms, can more effectively reduce the number of communication rounds.

1.1 Contributions

We consider the nonconvex FL problem (1) with \mathcal{M} being a compact smooth submanifold and allow for heterogeneous data distribution among clients. Our contributions are summarized as follows.

1) We propose a federated learning algorithm for solving (1) that is efficient in terms of both computation and communication. We employ stochastic Riemannian gradients and a projection operator to address manifold constraints, use local updates to reduce the communication frequency between clients and the server, and design correction terms to overcome client drift. In terms of server updates, our algorithm ensures feasibility of all global model iterates and is computationally efficient since it avoids the techniques used in [13] based on the exponential mapping and inverse exponential mapping for averaging local models on manifolds. For local updates, our algorithm constructs the correction terms locally without increasing communication costs. In comparison, the approach presented in [13] requires each client to transmit an additional local stochastic Riemannian gradient for constructing correction terms. Moreover, [13] necessitates parallel transport to position the correction terms on tangent spaces so that the exponential map can be applied to ensure the feasibility of local models, thereby increasing computational costs. In contrast, our algorithm utilizes a simple projection operator, effectively eliminating the need for parallel transport of correction terms.

2) Theoretically, we establish sub-linear convergence to a neighborhood of a first-order optimal solution and demonstrate how this neighborhood depends on the stochastic sampling variance and algorithm parameters. Our analysis introduces novel proof techniques that utilize the curvature of the manifolds and the properties of the loss functions to overcome the challenges posed by the nonconvexity of manifold constraints in the nonconvex FL scenario. Compared to the existing work

[13] where analytical results are limited to cases where either the number of local updates is one or the number of participating clients per communication round is one, our theoretical results allow for an arbitrary number of local updates and support full client participation.

3) Our algorithm demonstrates superior performance over alternative methods in the numerical experiments. In particular, it produces high-accuracy results for kPCA and low-rank matrix completion at a significantly lower communication and computation cost than alternative algorithms.

1.2 Related work

In this section, we first review federated learning algorithms for composite optimization with and without constraints. Then, we discuss FL algorithms with manifold constraints.

Composite FL in Euclidean space. Problem (1) can be viewed as a special case of composite FL where the loss function is a composition of f and the indicator function of \mathcal{M} . It is important to note that since the manifold is nonconvex, its indicator function is also nonconvex. Most existing composite FL methods can only handle convex constraints. The work [19] proposed a federated dual averaging method and established its convergence for a general loss function under bounded gradient assumptions, but only for quadratic losses under the bounded heterogeneity assumption that the degree of data heterogeneity among clients is bounded. In contrast, we make no assumptions about the similarity of data across clients. The fast federated dual averaging algorithm [20] extends the work in [19] by using both past gradient information and past model information in the local updates. However, the work [20] requires each client to transmit the local gradient as well as the local model, and it assumes bounded data heterogeneity. The work [21] introduces the federated Douglas-Rachford method, and the work [22] applies this algorithm to solve dual problems. Although these two methods avoid bounded data heterogeneity, they require an increasing number of local updates to ensure convergence, which reduces their practicality in federated learning. The recent work [23] proposes a communication-efficient FL algorithm that overcomes client drift by decoupling the proximal operator evaluation and the communication and shows that the method converges without any assumptions on data similarity.

Federated learning on manifolds. Since existing composite FL in Euclidean space only considers scenarios where the nonsmooth term in the loss functions is convex, these methods and their analyses cannot be directly applied to FL on manifolds. A typical challenge caused by the nonconvex manifold constraint is that the average of local models, each of which lies on the manifold, may not belong to the manifold. To address this issue, the work [13] introduced Riemannian federated SVRG (RFedSVRG), where the server maps the local models onto a tangent space, calculates an average, and then retracts the average back to the manifold. This process sequentially employs inverse exponential and exponential mappings. Moreover, RFedSVRG employs a correction term to overcome client drift but requires additional communication of local Riemannian gradients to construct the correction term. In addition, the method uses parallel transport to position the correction term, which increases the computation cost even further. The work [29] explores the differential privacy of RFedSVRG. Finally, the work [30] considers the specific manifold optimization problem that appears in PCA and investigates an ADMM-type method that penalizes the orthogonality constraint. However, this algorithm requires solving a subproblem to desired accuracy, which increases computational cost. The work [31] introduces a differentially private FL algorithm for solving PCA.

2 Preliminaries

The notation used in the paper is relatively standard and summarized in Appendix A.1. Below, we focus on introducing fundamental definitions and inequalities for optimization on manifolds.

2.1 Optimization on manifolds

Manifold optimization aims to minimize a real-valued function over a manifold, i.e., $\min_{x \in \mathcal{M}} f(x)$. Throughout the paper, we restrict our discussion to embedded submanifolds of the Euclidean space, where the associated topology coincides with the subspace topology of the Euclidean space. We refer to these as embedded submanifolds. Some examples of such manifolds include the Stiefel manifold, oblique manifold, and symplectic manifold [14]. In addition, we always take the Euclidean metric as the Riemannian metric. We define the tangent space of \mathcal{M} at point x as $T_x\mathcal{M}$, which contains all tangent vectors to \mathcal{M} at x , and the normal space as $N_x\mathcal{M}$ which is orthogonal to the tangent space.

With the definition of tangent space, we can define the Riemannian gradient that plays a central role in the characterization of optimality conditions and algorithm design for manifold optimization.

Definition 2.1 (Riemannian gradient $\text{grad}f(x)$). *The Riemannian gradient $\text{grad}f(x)$ of a function f at the point $x \in \mathcal{M}$ is the unique tangent vector that satisfies*

$$\langle \text{grad}f(x), \xi \rangle_x = df(x)[\xi], \quad \forall \xi \in T_x\mathcal{M},$$

where $\langle \cdot, \cdot \rangle_x$ is the Riemannian metric and df denotes the differential of function f .

For a submanifold \mathcal{M} , the Riemannian gradient $\text{grad}f(x)$ (under the Euclidean metric) can be computed as [14, Proposition 3.61]

$$\text{grad}f(x) = \mathcal{P}_{T_x\mathcal{M}}(\nabla f(x)),$$

where $\mathcal{P}_{T_x\mathcal{M}}(\nabla f(x))$ represents the orthogonal projection of $\nabla f(x)$ onto $T_x\mathcal{M}$. The Riemannian gradient $\text{grad}f(x)$ reduces to the Euclidean gradient $\nabla f(x)$ when \mathcal{M} is the Euclidean space $\mathbb{R}^{d \times k}$.

2.2 Proximal smoothness of \mathcal{M}

In our federated manifold learning algorithm, the server needs to fuse models that have undergone multiple rounds of local updates by the clients. Due to the nonconvexity of the manifold, the average of points on the manifold is not guaranteed to belong to the manifold. The tangent space-based exponential mapping or other retraction operations commonly used in manifold optimization are expensive in FL [13]. Specifically, the server needs to map the local models onto a tangent space using inverse exponential mapping, calculate an average on the tangent space, and then perform an exponential mapping to retract this average back onto the manifold. This exponential mapping, due to its dependency on the tangent space, also calls for parallel transport during the local updates when there are correction terms. To overcome this difficulty, we use a projection operator $\mathcal{P}_{\mathcal{M}}$ defined by

$$\mathcal{P}_{\mathcal{M}}(x) \in \underset{u \in \mathcal{M}}{\text{argmin}} \frac{1}{2} \|x - u\|^2 \quad (2)$$

to ensure the feasibility of manifold constraints. It is worth noting that $\mathcal{P}_{\mathcal{M}}$ can be regarded as a special retraction operator when restricted to the tangent space [32]. However, unlike a typical retraction operator, its domain is the entire space $\mathbb{R}^{d \times k}$, not just the tangent space, which enables a more practical averaging operation across clients in FL. Despite these advantageous properties, the nonconvex nature of the manifold means that $\mathcal{P}_{\mathcal{M}}(x)$ may be set-valued and non-Lipschitz, making the use and analysis of $\mathcal{P}_{\mathcal{M}}$ in the FL setting highly nontrivial. To tackle this, we introduce the concept of proximal smoothness that refers to a property of a closed set, including \mathcal{M} , where the projection becomes a singleton when the point is sufficiently close to the set.

Definition 2.2 ($\hat{\gamma}$ -proximal smoothness of \mathcal{M}). *For any $\hat{\gamma} > 0$, we define the $\hat{\gamma}$ -tube around \mathcal{M} as*

$$U_{\mathcal{M}}(\hat{\gamma}) := \{x : \text{dist}(x, \mathcal{M}) < \hat{\gamma}\},$$

where $\text{dist}(x, \mathcal{M}) := \min_{u \in \mathcal{M}} \|u - x\|$ is the Euclidean distance between x and \mathcal{M} . We say that \mathcal{M} is $\hat{\gamma}$ -proximally smooth if the projection operator $\mathcal{P}_{\mathcal{M}}(x)$ is a singleton whenever $x \in U_{\mathcal{M}}(\hat{\gamma})$.

It is worth noting that any compact smooth submanifold \mathcal{M} embedded in $\mathbb{R}^{d \times k}$ is a proximally smooth set [33, 34]. The constant $\hat{\gamma}$ can be calculated with the method of supporting principle for proximally smooth sets [35, 36]. For instance, the Stiefel manifold is 1-proximally smooth.

Assumption 2.3. *We assume that the proximal smoothness constant of \mathcal{M} is 2γ .*

With Assumption 2.3, we can ensure not only the uniqueness of the projection but also the Lipschitz continuity of the projection operator $\mathcal{P}_{\mathcal{M}}$ around \mathcal{M} , analogous to the non-expansiveness of projections under Euclidean convex constraints.

Lipschitz continuity of $\mathcal{P}_{\mathcal{M}}$. Define $\bar{U}_{\mathcal{M}}(\gamma) := \{x : \text{dist}(x, \mathcal{M}) \leq \gamma\}$ as the closure of $U_{\mathcal{M}}(\gamma)$. Following the proof in [33, Theorem 4.8], for a 2γ -proximally smooth \mathcal{M} , the projection operator $\mathcal{P}_{\mathcal{M}}$ is 2-Lipschitz continuous over $\bar{U}_{\mathcal{M}}(\gamma)$ such that

$$\|\mathcal{P}_{\mathcal{M}}(x) - \mathcal{P}_{\mathcal{M}}(y)\| \leq 2\|x - y\|, \quad \forall x, y \in \bar{U}_{\mathcal{M}}(\gamma). \quad (3)$$

Normal inequality. In the normal space $N_x\mathcal{M}$, we exploit the so-called normal inequality [33, 34]. Following [33], given a 2γ -proximally smooth \mathcal{M} , for any $x \in \mathcal{M}$ and $v \in N_x\mathcal{M}$, it holds that

$$\langle v, y - x \rangle \leq \frac{\|v\|}{4\gamma} \|y - x\|^2, \quad \forall y \in \mathcal{M}. \quad (4)$$

Intuitively, when x and y are close enough, the matrix $y - x$ is approximately in the tangent space, thus being nearly orthogonal to the normal space.

3 Proposed algorithm

In this section, we develop a novel algorithm for nonconvex federated learning on manifolds. The algorithm is inspired by the proximal FL algorithm for strongly convex problems in Euclidean space recently proposed in [23] but includes several non-trivial extensions. These include the use of Riemannian gradients and manifold projection operators and the ability to handle nonconvex loss functions, which call for a different convergence analysis.

Algorithm 1 Proposed algorithm

```

1: Input:  $R, \tau, \eta, \eta_g, \tilde{\eta} = \eta\eta_g\tau, x^1$ , and  $c_i^1 = 0$  for all  $i \in [n]$ 
2: for  $r = 1, 2, \dots, R$  do
3:   Client  $i$ 
4:   Set  $\hat{z}_{i,0}^r = \mathcal{P}_{\mathcal{M}}(x^r)$  and  $z_{i,0}^r = \mathcal{P}_{\mathcal{M}}(x^r)$ 
5:   for  $t = 0, 1, \dots, \tau - 1$  do
6:     Sample a mini-batch dataset  $\mathcal{B}_{i,t}^r \subseteq \mathcal{D}_i$  with  $|\mathcal{B}_{i,t}^r| = b$ 
7:     Update  $\text{grad}f_i(z_{i,t}^r; \mathcal{B}_{i,t}^r) = \frac{1}{b} \sum_{\mathcal{D}_{il} \in \mathcal{B}_{i,t}^r} \text{grad}f_{il}(z_{i,t}^r; \mathcal{D}_{il})$ 
8:     Update  $\hat{z}_{i,t+1}^r = \hat{z}_{i,t}^r - \eta (\text{grad}f_i(z_{i,t}^r; \mathcal{B}_{i,t}^r) + c_i^r)$ 
9:     Update  $z_{i,t+1}^r = \mathcal{P}_{\mathcal{M}}(\hat{z}_{i,t+1}^r)$ 
10:   end for
11:   Send  $\hat{z}_{i,\tau}^r$  to the server
12:   Server
13:   Update  $x^{r+1} = \mathcal{P}_{\mathcal{M}}(x^r) + \eta_g (\frac{1}{n} \sum_{i=1}^n \hat{z}_{i,\tau}^r - \mathcal{P}_{\mathcal{M}}(x^r))$ 
14:   Broadcast  $x^{r+1}$  to all the clients
15:   Client  $i$ 
16:   Receive  $x^{r+1}$  from the server
17:   Update  $c_i^{r+1} = \frac{1}{\eta_g\eta\tau} (\mathcal{P}_{\mathcal{M}}(x^r) - x^{r+1}) - \frac{1}{\tau} \sum_{t=0}^{\tau-1} \text{grad}f_i(z_{i,t}^r; \mathcal{B}_{i,t}^r)$ 
18: end for
19: Output:  $\mathcal{P}_{\mathcal{M}}(x^{R+1})$ 

```

3.1 Algorithm description

The per-client implementation of our algorithm is detailed in Algorithm 1. Similarly to the well-known FedAvg, it operates in a federated learning setting with one server and n clients. Each client i engages in τ steps of local updates before updating the server. We use r as the index of communication rounds and t as the index of local updates.

At any communication round r , client i downloads the global model x^r from the server and computes $\mathcal{P}_{\mathcal{M}}(x^r)$. Each client i updates two local variables, $\hat{z}_{i,t}^r$ and $z_{i,t}^r$, where $\hat{z}_{i,t}^r$ aggregates the Riemannian gradients from local updates, and $z_{i,t}^r = \mathcal{P}_{\mathcal{M}}(\hat{z}_{i,t}^r)$ ensures that Riemannian gradients can be computed at points on \mathcal{M} . The update of $\hat{z}_{i,t}^r$ is given in Line 8, where $\mathcal{B}_{i,t}^r$ is a mini-batch dataset and c_i^r is a correction term to eliminate client drift. After τ local updates, client i sends $\hat{z}_{i,\tau}^r$ to the server.

The server receives all $\hat{z}_{i,\tau}^r$, computes their average to form the global model x^{r+1} following Line 13, and broadcasts x^{r+1} to each client i that uses x^{r+1} to locally construct the correction term c_i^{r+1} .

In the proposed algorithm, each client i downloads x^r at the start of local updates and uploads $\hat{z}_{i,\tau}^r$ at the end of the local updates. Therefore, each communication round involves each client and the server exchanging only a single $d \times k$ matrix.

3.2 Algorithm intuition and innovations

To better understand the proposed algorithm, we present its equivalent and more compact form:

$$\begin{cases} \hat{\mathbf{z}}_{t+1}^r = \hat{\mathbf{z}}_t^r - \eta \left(\text{gradf}(\mathbf{z}_t^r; \mathcal{B}_t^r) + \frac{1}{\tau} \sum_{t=0}^{\tau-1} \overline{\text{gradf}}(\mathbf{z}_t^{r-1}; \mathcal{B}_t^{r-1}) - \frac{1}{\tau} \sum_{t=0}^{\tau-1} \text{gradf}(\mathbf{z}_t^{r-1}; \mathcal{B}_t^{r-1}) \right), \\ \mathbf{z}_{t+1}^r = \mathcal{P}_{\mathcal{M}}(\hat{\mathbf{z}}_{t+1}^r), \\ \mathbf{x}^{r+1} = \mathcal{P}_{\mathcal{M}}(\mathbf{x}^r) - \eta_g \eta \sum_{t=0}^{\tau-1} \overline{\text{gradf}}(\mathbf{z}_t^r; \mathcal{B}_t^r), \end{cases} \quad (5)$$

where the notations are in Appendix A.1. For the initialization of correction term, we set $\text{grad}f_i(z_{i,t}^0; \mathcal{B}_{i,t}^0) = 0$ for all t and i so that $\frac{1}{\tau} \sum_{t=0}^{\tau-1} \overline{\text{gradf}}(\mathbf{z}_t^0; \mathcal{B}_t^0) - \frac{1}{\tau} \sum_{t=0}^{\tau-1} \text{gradf}(\mathbf{z}_t^0; \mathcal{B}_t^0) = 0$, which coincides with the initialization $c_i^1 = 0$ in Algorithm 1. The equivalence between Algorithm 1 and (5) can be proved following the similar derivations in [23] and is therefore omitted.

With (5), we highlight the key properties and innovations of the proposed algorithm.

1) Recovery of the centralized algorithm in special cases. Substituting the definitions of \mathbf{x} , $\overline{\text{gradf}}(\mathbf{z}_t^r; \mathcal{B}_t^r)$, and $\tilde{\eta}$ into the last step in (5), we have

$$\mathcal{P}_{\mathcal{M}}(x^{r+1}) = \mathcal{P}_{\mathcal{M}} \left(\mathcal{P}_{\mathcal{M}}(x^r) - \underbrace{\tilde{\eta} \frac{1}{n\tau} \sum_{i=1}^n \sum_{t=0}^{\tau-1} (\text{grad}f_i(z_{i,t}^r; \mathcal{B}_{i,t}^r))}_{:=v^r} \right). \quad (6)$$

Thanks to the introduction of the variable $\hat{z}_{i,t}^r$ during the local updates for each client i in Algorithm 1, the server after averaging $\hat{z}_{i,t}^r$ obtains an accumulation of τ local Riemannian gradients across local updates and an average of the local Riemannian gradients across all clients. In the special case where $\tau = 1$ and $b = m_i$, i.e., with the local full Riemannian gradient for each client i , the update of (6) recovers the centralized projected Riemannian gradient descent (C-PRGD)

$$\tilde{x}^{r+1} := \mathcal{P}_{\mathcal{M}}(\mathcal{P}_{\mathcal{M}}(x^r) - \tilde{\eta} \text{grad}f(\mathcal{P}_{\mathcal{M}}(x^r))). \quad (7)$$

In our analysis, we will compare the sequence $\mathcal{P}_{\mathcal{M}}(x^{r+1})$ generated by our algorithm with the virtual iterate \tilde{x}^{r+1} to establish the convergence of our algorithm.

2) Feasibility of all iterates at a low computational cost. Our algorithm uses $\mathcal{P}_{\mathcal{M}}$ to obtain feasible solutions on the manifold, which is computationally more efficient than the commonly used exponential mapping. In fact, since the exponential mapping relies on a point on the manifold and the tangent space at that point, it cannot be directly used in our algorithm. In the local updates, it is difficult to perform exponential mapping on $\hat{\mathbf{z}}_{t+1}^r$ because $\hat{\mathbf{z}}_t^r$ is not on the manifold; see the first step in (5). As shown in [23], $\hat{\mathbf{z}}_{t+1}^r$ is essential for the server to obtain aggregated Riemannian gradients from n clients after τ local updates. Moreover, at the server, although $\mathcal{P}_{\mathcal{M}}(\mathbf{x}^r)$ is on the manifold, the aggregated direction does not lie in the tangent space at $\mathcal{P}_{\mathcal{M}}(\mathbf{x}^r)$. The algorithm suggested in [13] uses an exponential mapping to fuse local models. It needs to map the local models to a tangent space using the inverse exponential mapping and then retract the result back to the manifold, which is computationally expensive. Our use of $\mathcal{P}_{\mathcal{M}}$ on a point in the Euclidean space close to the manifold avoids these high computational costs, but creates new challenges for the analysis.

3) Overcoming client drift. Inspired by [23], we use a correction term c_i^r to address client drift. According to the first step of (5), the correction employs the idea of ‘‘variance reduction’’, which involves replacing the old local Riemannian gradient $\frac{1}{\tau} \sum_{t=0}^{\tau-1} \text{gradf}(\mathbf{z}_t^{r-1}; \mathcal{B}_t^{r-1})$ with the new one $\text{gradf}(\mathbf{z}_t^r; \mathcal{B}_t^r)$ in the average of all client Riemannian gradients $\frac{1}{\tau} \sum_{t=0}^{\tau-1} \overline{\text{gradf}}(\mathbf{z}_t^{r-1}; \mathcal{B}_t^{r-1})$, where the ‘‘variance’’ refers to the differences in Riemannian gradients among clients caused by data heterogeneity. Compared to [13], our correction improves communication and computation. The correction approach in [13] necessitates extra transmissions of local Riemannian gradients, while our correction term can be locally generated, leading to a significantly reduced communication overhead. Furthermore, the work [13] employs parallel transport to position the correction term with a specific tangent space for the exponential mapping to ensure local model feasibility. Our approach, which utilizes $\mathcal{P}_{\mathcal{M}}$, eliminates the need for parallel transport and reduces the computations per iteration even further.

4 Analysis

In this section, we analyze the convergence of the proposed Algorithm 1. Throughout the paper, we make the following assumptions, which are common in manifold optimization.

Assumption 4.1. Each $f_{il}(x; \mathcal{D}_{il}) : \mathbb{R}^{d \times k} \mapsto \mathbb{R}$ has \hat{L} -Lipschitz continuous gradient $\nabla f_{il}(x; \mathcal{D}_{il})$ on the convex hull of \mathcal{M} , denoted by $\text{conv}(\mathcal{M})$, i.e., for any $x, y \in \text{conv}(\mathcal{M})$, it holds that

$$\|\nabla f_{il}(x; \mathcal{D}_{il}) - \nabla f_{il}(y; \mathcal{D}_{il})\| \leq \hat{L}\|x - y\|. \quad (8)$$

With the compactness of \mathcal{M} , there exists a constant $D_f > 0$ such that the Euclidean gradient $\nabla f_{il}(x; \mathcal{D}_{il})$ of f_{il} is bounded by D_f , i.e., $\max_{i,l,x \in \mathcal{M}} \|\nabla f_{il}(x; \mathcal{D}_{il})\| \leq D_f$. It then follows from [27, Lemma 4.2] that there exists a constant $\hat{L} \leq L < \infty$ such that for any $x, y \in \mathcal{M}$,

$$\begin{aligned} f_{il}(y; \mathcal{D}_{il}) &\leq f_{il}(x; \mathcal{D}_{il}) + \langle \text{grad} f_{il}(x; \mathcal{D}_{il}), y - x \rangle + \frac{L}{2}\|x - y\|^2, \\ \|\text{grad} f_{il}(x; \mathcal{D}_{il}) - \text{grad} f_{il}(y; \mathcal{D}_{il})\| &\leq L\|x - y\|. \end{aligned}$$

To address the stochasticity introduced by the random sampling $\mathcal{B}_{i,t}^r$, we define \mathcal{F}_t^r as the σ -algebra generated by the set $\{\mathcal{B}_{i,\tilde{t}}^r \mid i \in [n], \tilde{r} \in [r], \tilde{t} \in [t-1]\}$ and make the following assumptions regarding the stochastic Riemannian gradients, similar to [37, Assumption 2].

Assumption 4.2. Each stochastic Riemannian gradient $\text{grad} f_i(z_{i,t}^r; \mathcal{B}_{i,t}^r)$ in Algorithm 1 satisfies

$$\begin{aligned} \mathbb{E} [\text{grad} f_i(z_{i,t}^r; \mathcal{B}_{i,t}^r) | \mathcal{F}_t^r] &= \text{grad} f_i(z_{i,t}^r), \\ \mathbb{E} [\|\text{grad} f_i(z_{i,t}^r; \mathcal{B}_{i,t}^r) - \text{grad} f_i(z_{i,t}^r)\|^2 | \mathcal{F}_t^r] &\leq \frac{\sigma^2}{b}. \end{aligned} \quad (9)$$

Considering the nonconvexity of f and the manifold constraints, we characterize the first-order optimality of (1). A point x^* is defined as a first-order optimal solution of (1) if $x^* \in \mathcal{M}$ and $\text{grad} f(x^*) = 0$. We employ the norm of $\mathcal{G}_{\tilde{\eta}}(\mathcal{P}_{\mathcal{M}}(x^r))$ as a suboptimality metric, defined as

$$\mathcal{G}_{\tilde{\eta}}(\mathcal{P}_{\mathcal{M}}(x^r)) := (\mathcal{P}_{\mathcal{M}}(x^r) - \tilde{x}^{r+1})/\tilde{\eta}, \quad (10)$$

and \tilde{x}^{r+1} defined in (7) is used only for analytical purposes. In optimization on Euclidean space such that $\mathcal{M} = \mathbb{R}^{d \times k}$, the quantity $\mathcal{G}_{\tilde{\eta}}(\mathcal{P}_{\mathcal{M}}(x^r))$ serves as a widely accepted metric to assess first-order optimality for nonconvex composite problems [38]. In optimization on manifold, we have $\mathcal{G}_{\tilde{\eta}}(\mathcal{P}_{\mathcal{M}}(x^r)) = 0$ if and only if $\text{grad} f(\mathcal{P}_{\mathcal{M}}(x^r)) = 0$ for any $\tilde{\eta} > 0$. Moreover, for a suitable $\tilde{\eta}$, we show that $1/2\|\text{grad} f(\mathcal{P}_{\mathcal{M}}(x^r))\| \leq \|\mathcal{G}_{\tilde{\eta}}(\mathcal{P}_{\mathcal{M}}(x^r))\| \leq 2\|\text{grad} f(\mathcal{P}_{\mathcal{M}}(x^r))\|$; see Lemmas A.1 and A.2. With $\mathcal{G}_{\tilde{\eta}}(\mathcal{P}_{\mathcal{M}}(x^r))$, we have the following theorem.

Theorem 4.3. Under Assumptions 2.3, 4.1, and 4.2, if the step sizes satisfy

$$\tilde{\eta} := \eta_g \eta \tau \leq \min \left\{ \frac{1}{24ML}, \frac{\gamma}{6D_f}, \frac{1}{D_f L_{\mathcal{P}}} \right\}, \quad \eta_g = \sqrt{n}, \quad (11)$$

where $M = \max\{\text{diam}(\mathcal{M})/\gamma, 2\}$, $\text{diam}(\mathcal{M}) = \max_{x,y \in \mathcal{M}} \|x - y\|$, $D_f = \max_{i,l,x \in \mathcal{M}} \|\nabla f_{il}(x; \mathcal{D}_{il})\|$, and $L_{\mathcal{P}} = \max_{x \in \bar{\mathcal{U}}_{\mathcal{M}}(\gamma)} \|D^2 \mathcal{P}_{\mathcal{M}}(x)\|$, then the sequence $\mathcal{P}_{\mathcal{M}}(x^r)$ generated by Algorithm 1 satisfies

$$\frac{1}{R} \sum_{r=1}^R \mathbb{E} \|\mathcal{G}_{\tilde{\eta}}(\mathcal{P}_{\mathcal{M}}(x^r))\|^2 \leq \frac{8\Omega^1}{\sqrt{n}\eta\tau R} + \frac{64\sigma^2}{n\tau b}, \quad (12)$$

where $\Omega^1 > 0$ is a constant related to initialization.

In Theorem 4.3, the first term on the right hand of (12) converges at a sub-linear rate, which is common for constrained nonconvex optimization [38, 39]. The second term is a constant error caused by the variance σ^2 of stochastic Riemannian gradients.

Theoretical contributions. The work [13] establishes convergence rates of $\mathcal{O}(1/R)$ for $\tau = 1$ and $\mathcal{O}(1/(\tau R))$ for $\tau > 1$ but only if a single client participates in the training per communication round. In contrast, our Theorem 4.3 achieves a rate of $\mathcal{O}(1/(\sqrt{n}\tau R))$ for $\tau > 1$ and full client participation.

Our theorem indicates that multiple local updates enable faster convergence, which distinguishes our algorithm from decentralized manifold optimization algorithms [6, 27] that limit clients to do a single local update. Our convergence analysis relies on several novel techniques. Specifically, we capitalize on the structure of \mathcal{M} and exploit the proximal smoothness of \mathcal{M} to guarantee the uniqueness of $\mathcal{P}_{\mathcal{M}}$ and Lipschitz continuity of $\mathcal{P}_{\mathcal{M}}$ within a tube around \mathcal{M} . Additionally, we carefully select the step sizes to ensure that the iterates remain close to \mathcal{M} , thus preserving the established properties throughout the iterations. Last but not least, we select an appropriate first-order optimality metric (see (10)) and jointly consider the properties of \mathcal{M} and the loss functions to establish some new inequalities for the convergence of this metric, given in Appendix.

5 Numerical experiments

In this section, we conduct numerical experiments on two applications on the Stiefel manifold: kPCA and the low rank matrix completion (LRMC). We compare with existing algorithms, including RFedavg, RFedprox, and RFedSVRG. RFedavg and RFedprox are direct extensions of FedAvg [24] and Fedprox [1]. For RFedSVRG, there are no theoretical guarantees when we set $\tau > 1$ and make all clients participate. In all alternative algorithms, the calculations of the exponential mapping, its inverse, and the parallel transport on the Stiefel manifold are needed. The exponential mapping has a closed-form expression but involves a matrix exponential [3], the inverse exponential mapping needs to solve a nonlinear matrix equation [16], and the parallel transport needs to solve a linear differential equation [40], all of which are computationally challenging. In their implementations, approximate versions of these mappings are used [13, 41, 42].

kPCA. Consider the kPCA problem

$$\underset{x \in \text{St}(d,k)}{\text{minimize}} f(x) = \frac{1}{n} \sum_{i=1}^n f_i(x), \quad f_i(x) = -\frac{1}{2} \text{tr}(x^T A_i^T A_i x),$$

where $\text{St}(d, k) = \{x \in \mathbb{R}^{d \times k} \mid x^T x = I_k\}$ denotes the Stiefel manifold, and $A_i^T A_i \in \mathbb{R}^{d \times d}$ is the covariance matrix of the local data $A_i \in \mathbb{R}^{p \times d}$ of client i . We conduct experiments where the matrix A_i is from the Mnist dataset. The specific experiment settings can be found in Appendix A.4.1.

In the first set of experiments, we compare with RFedavg, RFedprox, and RFedSVRG. Note that RFedSVRG requires each client to transmit two $d \times k$ matrices at each communication round, while our algorithm only transmits a single matrix. We use communication quantity to count the total number of $d \times k$ matrices that per client transmits to the server. We use the local full gradient ∇f_i to mitigate the effects of stochastic gradient noise. In Fig. 1, we set the number of local steps as $\tau = 10$ and the step size as $\eta = 1/\beta$ for all algorithms, where β is the square of the largest singular value of $\text{col}\{A_i\}_{i=1}^n$. For our algorithm, we set $\eta_g = 1$. It can be observed that RFedavg and RFedprox face the issue of client drift and have low accuracy. Both RFedSVRG and our algorithm can overcome the client drift, but our algorithm, though being similar in terms of communication rounds, is much faster in terms of both communication quantity and running time.

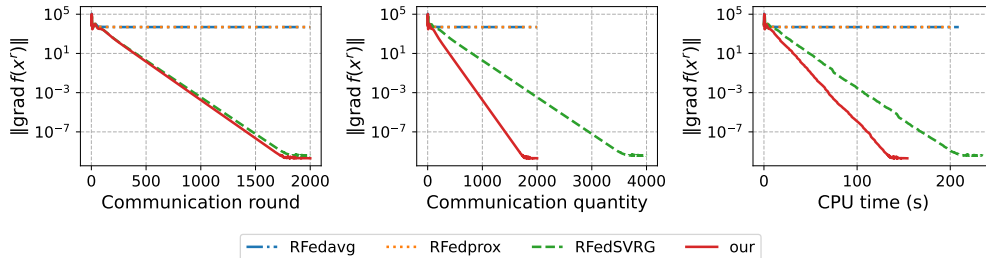


Figure 1: kPCA problem with Mnist dataset: Comparison on $\|\text{grad}f(x^r)\|$.

In the second set of experiments, we test the impact of τ . For all the algorithms, we set the step size $\eta = 1/\beta$ and $\tau \in \{10, 15, 20\}$. For our algorithm, we set $\eta_g = 1$. The experiment results are shown in Fig. 2. For all values of τ , our algorithm achieves better convergence and requires less communication quantity.

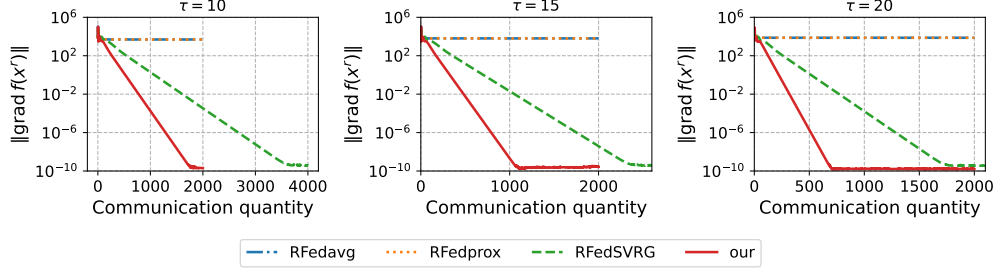


Figure 2: kPCA with Mnist dataset: The impacts of τ .

In addition, we test the impact of stochastic Riemannian gradients with different batch sizes. We set $\eta = 1/(20\beta)$. As shown in Fig. 3, our algorithm converges to a neighborhood due to the sampling noise and larger batch size leads to faster convergence.

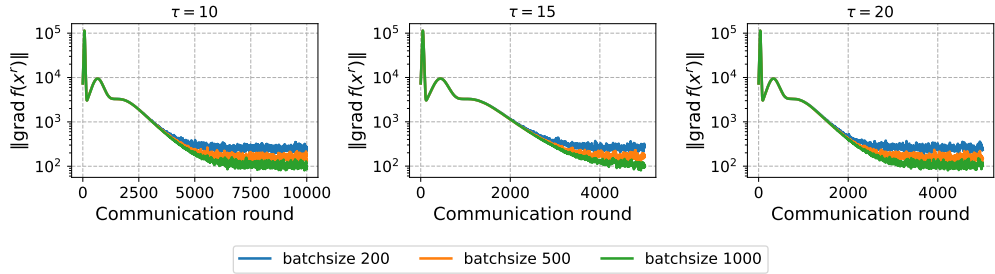


Figure 3: kPCA with Mnist dataset: The impacts of stochastic Riemannian gradients.

Low-rank matrix completion (LRMC). LRMC aims to recover a low-rank matrix $A \in \mathbb{R}^{d \times T}$ from its partial observations. Let Ω be the set of indices of known entries in A , the rank- k LRMC problem can be written as $\text{minimize}_{X \in \text{St}(d,k), V \in \mathbb{R}^{k \times T}} \frac{1}{2} \|\mathcal{P}_\Omega(XV - A)\|^2$, where the projection operator \mathcal{P}_Ω is defined in an entry-wise manner with $(\mathcal{P}_\Omega(A))_{l_1 l_2} = A_{l_1 l_2}$ if $(l_1, l_2) \in \Omega$ and 0 otherwise. In terms of the FL setting, we consider the case where the observed data matrix $\mathcal{P}_\Omega(A)$ is equally divided into n clients by columns, denoted by A_1, \dots, A_n . Then, the FL LRMC problem is

$$\text{minimize}_{X \in \text{St}(d,k)} \frac{1}{2n} \sum_{i=1}^n \|\mathcal{P}_{\Omega_i}(XV_i(X) - A_i)\|^2, \quad (13)$$

where Ω_i is the subset corresponding to client i in Ω and $V_i(X) := \text{argmin}_V \|\mathcal{P}_{\Omega_i}(XV - A_i)\|$. In the experiments, we set $T = 1000$, $d = 100$, $k = 2$, $n = 10$, and use the local full gradients. The other settings can be found in Appendix A.4.2.

The numerical comparisons with RFedavg, RFedprox, and RFedSVRG are presented in Figs. 4. Our algorithm and RFedSVRG achieve similar convergence for communication rounds, but our algorithm converges faster than RFedSVRG in terms of communication quantity and running time.

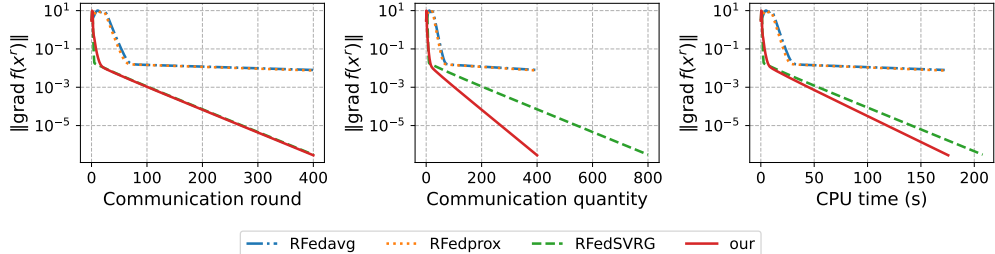


Figure 4: LRMC: Comparison on $\|\text{grad} f(x^r)\|$.

6 Conclusions and limitations

This paper addresses the challenges of FL on compact smooth submanifolds. We introduce a novel algorithm that enables full client participation, local updates, and heterogeneous data distributions. By leveraging stochastic Riemannian gradients and a manifold projection operator, our method enhances computational and communication efficiency while mitigating client drift. By exploiting the manifold structure and properties of the loss function, we prove sub-linear convergence to a neighborhood of a first-order stationary point. Numerical experiments show a superior performance of our algorithm in terms of computational and communication costs compared to the state-of-the-art.

Limitations. Our paper motivates several questions for further investigation. First, the absence of closed-form solutions for the projection operator $\mathcal{P}_{\mathcal{M}}$ for certain manifolds necessitates exploring methods to calculate projections approximately. Additionally, our step-size selection relies on the proximal smoothness constant γ , underscoring the need for estimating γ either off-line for specific manifolds or adaptively on-line. Furthermore, designing algorithms for partial participation and devising corresponding client-drift correction mechanisms require further investigation.

References

- [1] Tian Li, Anit Kumar Sahu, Manzil Zaheer, Maziar Sanjabi, Ameet Talwalkar, and Virginia Smith. Federated optimization in heterogeneous networks. *Proceedings of Machine Learning and Systems*, 2:429–450, 2020.
- [2] Peter Kairouz, H Brendan McMahan, Brendan Avent, Aurélien Bellet, Mehdi Bennis, Arjun Nitin Bhagoji, Kallista Bonawitz, Zachary Charles, Graham Cormode, Rachel Cummings, et al. Advances and open problems in federated learning. *Foundations and Trends® in Machine Learning*, 14(1–2):1–210, 2021.
- [3] Shixiang Chen, Shiqian Ma, Anthony Man-Cho So, and Tong Zhang. Proximal gradient method for nonsmooth optimization over the stiefel manifold. *SIAM Journal on Optimization*, 30(1):210–239, 2020.
- [4] Lei Wang and Xin Liu. Decentralized optimization over the Stiefel manifold by an approximate augmented lagrangian function. *IEEE Transactions on Signal Processing*, 70:3029–3041, 2022.
- [5] Haishan Ye and Tong Zhang. DeEPCA: Decentralized exact PCA with linear convergence rate. *Journal of Machine Learning Research*, 22(238):1–27, 2021.
- [6] Shixiang Chen, Alfredo Garcia, Mingyi Hong, and Shahin Shahrampour. Decentralized Riemannian gradient descent on the Stiefel manifold. In *International Conference on Machine Learning*, pages 1594–1605. PMLR, 2021.
- [7] Nicolas Boumal and P-A Absil. Low-rank matrix completion via preconditioned optimization on the Grassmann manifold. *Linear Algebra and its Applications*, 475:200–239, 2015.
- [8] Hiroyuki Kasai, Pratik Jawanpuria, and Bamdev Mishra. Riemannian adaptive stochastic gradient algorithms on matrix manifolds. In *International Conference on Machine Learning*, pages 3262–3271. PMLR, 2019.
- [9] Nilesh Tripuraneni, Chi Jin, and Michael Jordan. Provable meta-learning of linear representations. In *International Conference on Machine Learning*, pages 10434–10443. PMLR, 2021.
- [10] Nikolaos Dimitriadis, Pascal Frossard, and François Fleuret. Pareto manifold learning: Tackling multiple tasks via ensembles of single-task models. In *International Conference on Machine Learning*, pages 8015–8052. PMLR, 2023.
- [11] German Magai. Deep neural networks architectures from the perspective of manifold learning. In *2023 IEEE 6th International Conference on Pattern Recognition and Artificial Intelligence (PRAI)*, pages 1021–1031. IEEE, 2023.
- [12] Thomas Yerxa, Yilun Kuang, Eero Simoncelli, and SueYeon Chung. Learning efficient coding of natural images with maximum manifold capacity representations. *Advances in Neural Information Processing Systems*, 36:24103–24128, 2023.
- [13] Jiaxiang Li and Shiqian Ma. Federated learning on Riemannian manifolds. *arXiv preprint arXiv:2206.05668*, 2022.
- [14] Nicolas Boumal. *An introduction to optimization on smooth manifolds*. Cambridge University Press, 2023.
- [15] Jiang Hu, Xin Liu, Zaiwen Wen, and Yaxiang Yuan. A brief introduction to manifold optimization. *Journal of the Operations Research Society of China*, 8:199–248, 2020.
- [16] Ralf Zimmermann and Knut Huper. Computing the Riemannian logarithm on the Stiefel manifold: Metrics, methods, and performance. *SIAM Journal on Matrix Analysis and Applications*, 43(2):953–980, 2022.
- [17] Xiang Li, Kaixuan Huang, Wenhao Yang, Shusen Wang, and Zhihua Zhang. On the convergence of FedAvg on non-iid data. In *International Conference on Learning Representations*, 2019.
- [18] Sai Praneeth Karimireddy, Satyen Kale, Mehryar Mohri, Sashank Reddi, Sebastian Stich, and Ananda Theertha Suresh. Scaffold: Stochastic controlled averaging for federated learning. In *International Conference on Machine Learning*, pages 5132–5143, 2020.
- [19] Honglin Yuan, Manzil Zaheer, and Sashank Reddi. Federated composite optimization. In *International Conference on Machine Learning*, pages 12253–12266, 2021.

- [20] Yajie Bao, Michael Crawshaw, Shan Luo, and Mingrui Liu. Fast composite optimization and statistical recovery in federated learning. In *International Conference on Machine Learning*, pages 1508–1536, 2022.
- [21] Quoc Tran Dinh, Nhan H Pham, Dzung Phan, and Lam Nguyen. FedDR—randomized Douglas-Rachford splitting algorithms for nonconvex federated composite optimization. *Advances in Neural Information Processing Systems*, 34:30326–30338, 2021.
- [22] Han Wang, Siddhartha Marella, and James Anderson. FedADMM: A federated primal-dual algorithm allowing partial participation. In *2022 IEEE 61st Conference on Decision and Control (CDC)*, pages 287–294, 2022.
- [23] Jiaojiao Zhang, Jiang Hu, and Mikael Johansson. Composite federated learning with heterogeneous data. In *ICASSP 2024-2024 IEEE International Conference on Acoustics, Speech and Signal Processing (ICASSP)*, pages 8946–8950. IEEE, 2024.
- [24] Brendan McMahan, Eider Moore, Daniel Ramage, Seth Hampson, and Blaise Aguera y Arcas. Communication-efficient learning of deep networks from decentralized data. In *Artificial Intelligence and Statistics*, pages 1273–1282, 2017.
- [25] Sai Praneeth Karimireddy, Martin Jaggi, Satyen Kale, Mehryar Mohri, Sashank J Reddi, Sebastian U Stich, and Ananda Theertha Suresh. Mime: Mimicking centralized stochastic algorithms in federated learning. *arXiv preprint arXiv:2008.03606*, 2020.
- [26] Aritra Mitra, Rayana Jaafar, George J Pappas, and Hamed Hassani. Linear convergence in federated learning: Tackling client heterogeneity and sparse gradients. *Advances in Neural Information Processing Systems*, 34:14606–14619, 2021.
- [27] Kangkang Deng and Jiang Hu. Decentralized projected Riemannian gradient method for smooth optimization on compact submanifolds. *arXiv preprint arXiv:2304.08241*, 2023.
- [28] Jun Chen, Haishan Ye, Mengmeng Wang, Tianxin Huang, Guang Dai, Ivor Tsang, and Yong Liu. Decentralized Riemannian conjugate gradient method on the Stiefel manifold. In *The Twelfth International Conference on Learning Representations*, 2024.
- [29] Zhenwei Huang, Wen Huang, Pratik Jawanpuria, and Bamdev Mishra. Federated learning on Riemannian manifolds with differential privacy. *arXiv preprint arXiv:2404.10029*, 2024.
- [30] Tung-Anh Nguyen, Jiayu He, Long Tan Le, Wei Bao, and Nguyen H Tran. Federated PCA on Grassmann manifold for anomaly detection in iot networks. In *IEEE INFOCOM 2023-IEEE Conference on Computer Communications*, pages 1–10. IEEE, 2023.
- [31] Andreas Grammenos, Rodrigo Mendoza Smith, Jon Crowcroft, and Cecilia Mascolo. Federated principal component analysis. *Advances in Neural Information Processing Systems*, 33:6453–6464, 2020.
- [32] P-A Absil and Jérôme Malick. Projection-like retractions on matrix manifolds. *SIAM Journal on Optimization*, 22(1):135–158, 2012.
- [33] Francis H Clarke, Ronald J Stern, and Peter R Wolenski. Proximal smoothness and the lower-C2 property. *Journal of Convex Analysis*, 2(1-2):117–144, 1995.
- [34] Damek Davis, Dmitriy Drusvyatskiy, and Zhan Shi. Stochastic optimization over proximally smooth sets. *arXiv preprint arXiv:2002.06309*, 2020.
- [35] MV Balashov. Nonconvex optimization. *Control theory (additional chapters): tutorial. Moscow: Lenand*, 2019.
- [36] MV Balashov and AA Tremba. Error bound conditions and convergence of optimization methods on smooth and proximally smooth manifolds. *Optimization*, 71(3):711–735, 2022.
- [37] Pan Zhou, Xiao-Tong Yuan, and Jiashi Feng. Faster first-order methods for stochastic nonconvex optimization on Riemannian manifolds. In *The 22nd International Conference on Artificial Intelligence and Statistics*, pages 138–147. PMLR, 2019.
- [38] Sashank J Reddi, Suvrit Sra, Barnabas Poczos, and Alexander J Smola. Proximal stochastic methods for nonsmooth nonconvex finite-sum optimization. *Advances in Neural Information Processing Systems*, 29, 2016.
- [39] Manzil Zaheer, Sashank Reddi, Devendra Sachan, Satyen Kale, and Sanjiv Kumar. Adaptive methods for nonconvex optimization. *Advances in neural information processing systems*, 31, 2018.

- [40] Alan Edelman, Tomás A Arias, and Steven T Smith. The geometry of algorithms with orthogonality constraints. *SIAM journal on Matrix Analysis and Applications*, 20(2):303–353, 1998.
- [41] Nicolas Boumal, Bamdev Mishra, P-A Absil, and Rodolphe Sepulchre. Manopt, a Matlab toolbox for optimization on manifolds. *The Journal of Machine Learning Research*, 15(1):1455–1459, 2014.
- [42] James Townsend, Niklas Koep, and Sebastian Weichwald. Pymanopt: A python toolbox for optimization on manifolds using automatic differentiation. *Journal of Machine Learning Research*, 17(137):1–5, 2016.
- [43] Robert L Foote. Regularity of the distance function. *Proceedings of the American Mathematical Society*, 92(1):153–155, 1984.
- [44] Maxence Noble, Aurélien Bellet, and Aymeric Dieuleveut. Differentially private federated learning on heterogeneous data. In *International Conference on Artificial Intelligence and Statistics*, pages 10110–10145, 2022.

A Appendix

A.1 Notations

We use I_k to denote a $k \times k$ identity matrix. We use $\|\cdot\|$ to denote Frobenius norm and $\text{tr}(\cdot)$ to denote the trace of a matrix. For a set \mathcal{B} , we use $|\mathcal{B}|$ to denote the cardinality. For a random variable v , we use $\mathbb{E}[v]$ to denote the expectation and $\mathbb{E}[v|\mathcal{F}]$ to denote the expectation given event \mathcal{F} . For an integer n , we use $[n]$ to denote the set $\{1, \dots, n\}$. For two matrices $x, y \in \mathbb{R}^{d \times k}$, we define their Euclidean inner product as $\langle x, y \rangle := \sum_{i=1}^d \sum_{j=1}^k x_{ij} y_{ij}$. For matrices $z_1, \dots, z_n \in \mathbb{R}^{d \times k}$, we use $\mathbf{z} := \text{col}\{z_i\}_{i=1}^n := [z_1; \dots; z_n] \in \mathbb{R}^{nd \times k}$ to denote the vertical stack of all matrices. The bold notations $\widehat{\mathbf{z}}$, \mathbf{c} , and $\mathbf{\Lambda}$ are defined similarly. Specifically, for a matrix $x \in \mathbb{R}^{d \times k}$, we define $\mathbf{x} := \text{col}\{x\}_{i=1}^n := [x; \dots; x] \in \mathbb{R}^{nd \times k}$. We use r to denote the index of the communication round and t to denote the index of local updates. Given the local Riemannian gradient $\text{grad}f_i(z_{i,t}^r; \mathcal{B}_{i,t}^r)$ at point $z_{i,t}^r$ with the mini-batch dataset $\mathcal{B}_{i,t}^r$, we define the stack of Riemannian gradients as $\overline{\text{gradf}}(\mathbf{z}_t^r; \mathcal{B}_t^r) := \text{col}\{\text{grad}f_i(z_{i,t}^r; \mathcal{B}_{i,t}^r)\}_{i=1}^n$ and the stack of average local Riemannian gradients as $\text{gradf}(\mathbf{z}_t^r; \mathcal{B}_t^r) := \text{col}\{\frac{1}{n} \sum_{i=1}^n \text{grad}f_i(z_{i,t}^r; \mathcal{B}_{i,t}^r)\}_{i=1}^n$. Given $\text{col}\{z_i\}_{i=1}^n$ and $\mathcal{P}_{\mathcal{M}}(z_i)$, we define $\mathcal{P}_{\mathcal{M}}(\text{col}\{z_i\}_{i=1}^n) = \text{col}\{\mathcal{P}_{\mathcal{M}}(z_i)\}_{i=1}^n$.

We analyze the proposed algorithm using the Lyapunov function Ω^r defined by

$$\Omega^r := f(\mathcal{P}_{\mathcal{M}}(x^r)) - f^* + \frac{1}{n\bar{\eta}} \|\mathbf{\Lambda}^r - \overline{\mathbf{\Lambda}}^r\|^2, \quad (14)$$

where f^* is the optimal value of problem (1) and we define

$$\mathbf{\Lambda}^r := \eta(\tau \text{gradf}(\mathcal{P}_{\mathcal{M}}(\mathbf{x}^r)) + \sum_{t=0}^{\tau-1} \overline{\text{gradf}}(\mathbf{z}_t^{r-1}; \mathcal{B}_t^{r-1}) - \sum_{t=0}^{\tau-1} \text{gradf}(\mathbf{z}_t^{r-1}; \mathcal{B}_t^{r-1}))$$

and $\overline{\mathbf{\Lambda}}^r := \text{col}\{\frac{1}{n} \sum_{i=1}^n \mathbf{\Lambda}_i^r\}_{i=1}^n$.

The Lyapunov function consists of two parts: to bound the suboptimality of the global model $\mathcal{P}_{\mathcal{M}}(x^r)$ and the reduction of ‘‘variance’’ among clients, respectively.

A.2 Preliminary lemmas

Let us start with the following lemma on the global-like Lipschitz-continuity property of $\mathcal{P}_{\mathcal{M}}$.

Lemma A.1. *There exists a constant $M > 0$ such that for any $x \in \mathcal{M}$,*

$$\|\mathcal{P}_{\mathcal{M}}(x+u) - x\| \leq M\|u\|. \quad (15)$$

Proof. Let us consider two cases:

- $\|u\| \geq \gamma$: Since $\mathcal{P}_{\mathcal{M}}(x+u)$ and x belong to \mathcal{M} , we have

$$\|\mathcal{P}_{\mathcal{M}}(x+u) - x\| \leq \text{diam}(\mathcal{M}) \leq \frac{\text{diam}(\mathcal{M})}{\gamma} \|u\|,$$

where $\text{diam}(\mathcal{M}) := \max_{x,y \in \mathcal{M}} \|x - y\|$ is the diameter of \mathcal{M} .

- $\|u\| \leq \gamma$: By the 2-Lipschitz continuity of $\mathcal{P}_{\mathcal{M}}$ over $\overline{U}_{\mathcal{M}}(\gamma)$ in (3), we have

$$\|\mathcal{P}_{\mathcal{M}}(x+u) - x\| \leq 2\|u\|.$$

Setting $M := \max\left\{\frac{\text{diam}(\mathcal{M})}{\gamma}, 2\right\}$, we complete the proof. \square

In the following, we show the reasonableness of the suboptimality metric $\|\mathcal{G}_{\bar{\eta}}(\cdot)\|$.

Lemma A.2. *Consider $\mathcal{G}_{\bar{\eta}}(\cdot)$ defined by (10). Then, for any $x \in \mathcal{M}$, it holds that*

$$\text{grad}f(x) = 0 \quad \text{if and only if} \quad \mathcal{G}_{\bar{\eta}}(x) = 0.$$

In addition, under Assumptions 2.3 and 4.1, if $\bar{\eta} \leq \min\left\{\frac{\gamma}{D_f}, \frac{1}{D_f L_{\mathcal{P}}}\right\}$ with $L_{\mathcal{P}}$ being the smoothness constant of $D^2\mathcal{P}_{\mathcal{M}}(\cdot)$ over $\overline{U}_{\mathcal{M}}(\gamma)$, it holds that

$$\|\text{grad}f(x)\| \leq 2\|\mathcal{G}_{\bar{\eta}}(x)\|. \quad (16)$$

Proof. If $\text{grad}f(x) = 0$, it follows directly from the definition of $\mathcal{G}_{\tilde{\eta}}(\cdot)$ that $\mathcal{G}_{\tilde{\eta}}(x) = 0$. Conversely, if $\mathcal{G}_{\tilde{\eta}}(x) = 0$, we have

$$x = \mathcal{P}_{\mathcal{M}}(x - \tilde{\eta}\text{grad}f(x)) := \underset{y \in \mathcal{M}}{\text{argmin}} \|y - x + \tilde{\eta}\text{grad}f(x)\|^2.$$

It follows from the optimality of x that $0 = P_{T_x \mathcal{M}}(\tilde{\eta}\text{grad}f(x))$, which implies that $\text{grad}f(x) = 0$.

With [43, Lemma], $\mathcal{P}_{\mathcal{M}}(\cdot)$ is sufficiently smooth over $\bar{U}_{\mathcal{M}}(\gamma)$. Let us define $L_{\mathcal{P}} := \max_{x \in \bar{U}_{\mathcal{M}}(\gamma)} \|D^2 \mathcal{P}_{\mathcal{M}}(x)\|$, then we have

$$\begin{aligned} \|\mathcal{G}_{\tilde{\eta}}(x)\| &= \frac{1}{\tilde{\eta}} \|x - \mathcal{P}_{\mathcal{M}}(x - \tilde{\eta}\text{grad}f(x))\| \\ &\geq \|\text{grad}f(x)\| - \frac{1}{2} L_{\mathcal{P}} \tilde{\eta} \|\text{grad}f(x)\|^2 \\ &\geq \frac{1}{2} \|\text{grad}f(x)\|, \end{aligned}$$

where we use $\tilde{\eta} \leq \frac{\gamma}{D_f}$ in the first inequality and $\tilde{\eta} \leq \frac{1}{L_{\mathcal{P}} D_f}$ in the second inequality. This gives (16). \square

To prove Theorem 4.3, we use the following lemma to establish a recursion on the second term on $\mathbf{\Lambda}^r$ in the Lyapunov function.

Lemma A.3. *Under Assumptions 2.3, 4.1, and 4.2, if $\tilde{\eta} \leq \min \left\{ \frac{\eta_g}{16L}, \frac{\gamma \eta_g}{2D_f} \right\}$, we have*

$$\begin{aligned} &\frac{1}{n} \mathbb{E} \|\mathbf{\Lambda}^{r+1} - \bar{\mathbf{\Lambda}}^{r+1}\|^2 - 2\eta^2 \tau^2 L^2 \mathbb{E} \|\mathcal{P}_{\mathcal{M}}(x^{r+1}) - \mathcal{P}_{\mathcal{M}}(x^r)\|^2 \quad (17) \\ &\leq \frac{1}{n} 4\eta^2 \tau L^2 \left(3nM^2 \tau^3 \eta^2 \|\text{grad}f(\mathcal{P}_{\mathcal{M}}(x^r))\|^2 + 9\tau \mathbb{E} \|\mathbf{\Lambda}^r - \bar{\mathbf{\Lambda}}^r\|^2 + 18n\tau^2 \eta^2 \frac{\sigma^2}{b} \right) + \frac{1}{n} 4\eta^2 n^2 \tau^2 \frac{\sigma^2}{n\tau b}. \end{aligned}$$

Proof. As a first step, we bound the drift error $\|z_{i,t+1}^r - \mathcal{P}_{\mathcal{M}}(x^r)\|^2$ that is caused by the local updates. If $\tau = 1$, the error is zero since $z_{i,t}^r = \mathcal{P}_{\mathcal{M}}(x^r)$. When $\tau \geq 2$, repeating the local updates for t steps and substituting $\tilde{z}_{i,0}^r = \mathcal{P}_{\mathcal{M}}(x^r)$ and $z_{i,t+1}^r = \mathcal{P}_{\mathcal{M}}(\tilde{z}_{i,t+1}^r)$, we have

$$\mathbb{E} \|z_{i,t+1}^r - \mathcal{P}_{\mathcal{M}}(x^r)\|^2 = \mathbb{E} \left\| \mathcal{P}_{\mathcal{M}} \left(\mathcal{P}_{\mathcal{M}}(x^r) - \eta \sum_{\ell=0}^t (\text{grad}f_i(z_{i,\ell}^r; \mathcal{B}_{i,\ell}^r) + c_i^r) \right) - \mathcal{P}_{\mathcal{M}}(x^r) \right\|^2. \quad (18)$$

To bound the right-hand side of (18), we compare our algorithm with the exact C-PRGD step given in (7) under the step size $(t+1)\eta$

$$\tilde{x}_{\text{C-PRGD}}^{r+1} := \mathcal{P}_{\mathcal{M}}(\mathcal{P}_{\mathcal{M}}(x^r) - (t+1)\eta \text{grad}f(\mathcal{P}_{\mathcal{M}}(x^r))).$$

It follows from (15) that

$$\|\tilde{x}_{\text{C-PRGD}}^{r+1} - \mathcal{P}_{\mathcal{M}}(x^r)\| \leq M\tau\eta \|\text{grad}f(\mathcal{P}_{\mathcal{M}}(x^r))\|.$$

Then from (18) we have

$$\begin{aligned} &\mathbb{E} \|z_{i,t+1}^r - \mathcal{P}_{\mathcal{M}}(x^r)\|^2 \quad (19) \\ &= \mathbb{E} \left\| \mathcal{P}_{\mathcal{M}} \left(\mathcal{P}_{\mathcal{M}}(x^r) - \eta \sum_{\ell=0}^t (\text{grad}f_i(z_{i,\ell}^r; \mathcal{B}_{i,\ell}^r) + c_i^r) \right) - \tilde{x}_{\text{C-PRGD}}^{r+1} + \tilde{x}_{\text{C-PRGD}}^{r+1} - \mathcal{P}_{\mathcal{M}}(x^r) \right\|^2 \\ &\leq 2\mathbb{E} \underbrace{\left\| \mathcal{P}_{\mathcal{M}} \left(\mathcal{P}_{\mathcal{M}}(x^r) - \eta \sum_{\ell=0}^t (\text{grad}f_i(z_{i,\ell}^r; \mathcal{B}_{i,\ell}^r) + c_i^r) \right) - \tilde{x}_{\text{C-PRGD}}^{r+1} \right\|^2}_{(I)} + 2M^2 \tau^2 \eta^2 \|\text{grad}f(\mathcal{P}_{\mathcal{M}}(x^r))\|^2, \end{aligned}$$

where we use $\|a+b\|^2 \leq 2\|a\|^2 + 2\|b\|^2$ in the inequality.

To bound the term (I) on the right hand of (19), from $\tilde{\eta} \leq \frac{\gamma\eta a}{2D_f}$ and $\max_{i,l,x \in \mathcal{M}} \|\nabla f_{il}(x; \mathcal{D}_{il})\| \leq D_f$, we have

$$\left\| \eta \sum_{\ell=0}^t (\text{grad} f_i(z_{i,\ell}^r; \mathcal{B}_{i,\ell}^r) + c_i^r) \right\| \leq \gamma.$$

Thus, by substituting definition of $\tilde{x}_{\text{C-PRGD}}^{r+1}$, we can invoke the 2-Lipschitz continuity of $\mathcal{P}_{\mathcal{M}}$ over $\bar{U}_{\mathcal{M}}(\gamma)$ given in (3) and get

$$\begin{aligned} \text{(I)} &= 2\mathbb{E} \left\| \mathcal{P}_{\mathcal{M}}(\mathcal{P}_{\mathcal{M}}(x^r) - \eta \sum_{\ell=0}^t (\text{grad} f_i(z_{i,\ell}^r; \mathcal{B}_{i,\ell}^r) + c_i^r)) \right. \\ &\quad \left. - \mathcal{P}_{\mathcal{M}}(\mathcal{P}_{\mathcal{M}}(x^r) - (t+1)\eta \text{grad} f(\mathcal{P}_{\mathcal{M}}(x^r))) \right\|^2 \\ &\leq 4\mathbb{E} \left\| \eta \sum_{\ell=0}^t (\text{grad} f_i(z_{i,\ell}^r; \mathcal{B}_{i,\ell}^r) + c_i^r - \text{grad} f(\mathcal{P}_{\mathcal{M}}(x^r))) \right\|^2. \end{aligned} \quad (20)$$

Next, to bound the right-hand side of (20) we rewrite it in terms of $\|\Lambda^r - \bar{\Lambda}^r\|^2$ by substituting the definition of the c_i^r given in (5)

$$\begin{aligned} \text{(I)} &\leq 4\mathbb{E} \left\| \eta \sum_{\ell=0}^t (\text{grad} f_i(z_{i,\ell}^r; \mathcal{B}_{i,\ell}^r) - \text{grad} f_i(\mathcal{P}_{\mathcal{M}}(x^r))) \right. \\ &\quad \left. + \text{grad} f_i(\mathcal{P}_{\mathcal{M}}(x^r)) + \frac{1}{\tau} \sum_{t=0}^{\tau-1} \frac{1}{n} \sum_{i=1}^n \text{grad} f_i(z_{i,t}^{r-1}; \mathcal{B}_{i,t}^{r-1}) \right. \\ &\quad \left. - \frac{1}{\tau} \sum_{t=0}^{\tau-1} \text{grad} f_i(z_{i,t}^{r-1}; \mathcal{B}_{i,t}^{r-1}) - \text{grad} f(\mathcal{P}_{\mathcal{M}}(x^r)) \right\|^2 \\ &= 4\mathbb{E} \left\| \eta \sum_{\ell=0}^t (\text{grad} f_i(z_{i,\ell}^r; \mathcal{B}_{i,\ell}^r) - \text{grad} f_i(\mathcal{P}_{\mathcal{M}}(x^r))) + \frac{1}{\eta\tau} (\Lambda_i^r - \bar{\Lambda}^r) \right\|^2 \\ &\leq \underbrace{8\mathbb{E} \left\| \eta \sum_{\ell=0}^t (\text{grad} f_i(z_{i,\ell}^r; \mathcal{B}_{i,\ell}^r) - \text{grad} f_i(\mathcal{P}_{\mathcal{M}}(x^r))) \right\|^2}_{\text{(II)}} + 8\mathbb{E} \left\| \frac{t+1}{\tau} \Lambda_i^r - \frac{t+1}{\tau} \bar{\Lambda}^r \right\|^2. \end{aligned} \quad (21)$$

Next, for the term (II), substituting Assumption 4.2 yields

$$\begin{aligned} \text{(II)} &= 8\mathbb{E} \left\| \eta \sum_{\ell=0}^t (\text{grad} f_i(z_{i,\ell}^r; \mathcal{B}_{i,\ell}^r) - \text{grad} f_i(z_{i,\ell}^r) + \text{grad} f_i(z_{i,\ell}^r) - \text{grad} f_i(\mathcal{P}_{\mathcal{M}}(x^r))) \right\|^2 \\ &\leq 16(t+1)^2 \mathbb{E} \left\| \frac{\eta}{t+1} \sum_{\ell=0}^t (\text{grad} f_i(z_{i,\ell}^r; \mathcal{B}_{i,\ell}^r) - \text{grad} f_i(z_{i,\ell}^r)) \right\|^2 \\ &\quad + 16\mathbb{E} \left\| \eta \sum_{\ell=0}^t (\text{grad} f_i(z_{i,\ell}^r) - \text{grad} f_i(\mathcal{P}_{\mathcal{M}}(x^r))) \right\|^2. \end{aligned} \quad (22)$$

For the first term can be handled by the fact [44, Corollary C.1] that

$$\begin{aligned} &16(t+1)^2 \eta^2 \mathbb{E} \left\| \frac{1}{t+1} \sum_{\ell=0}^t (\text{grad} f_i(z_{i,\ell}^r; \mathcal{B}_{i,\ell}^r) - \text{grad} f_i(z_{i,\ell}^r)) \right\|^2 \\ &= \frac{16(t+1)^2 \eta^2}{(t+1)^2} \sum_{\ell=0}^t \mathbb{E} \left[\mathbb{E} \left[\left\| (\text{grad} f_i(z_{i,\ell}^r; \mathcal{B}_{i,\ell}^r) - \text{grad} f_i(z_{i,\ell}^r)) \right\|^2 \middle| \mathcal{F}_t^r \right] \right] \leq \frac{1}{t+1} \frac{\sigma^2}{b}. \end{aligned} \quad (23)$$

Combining (22), (23), and (21), we have

$$\text{(I)} \leq 16(t+1)\eta^2 L^2 \sum_{\ell=0}^t \mathbb{E} \|z_{i,\ell}^r - \mathcal{P}_{\mathcal{M}}(x^r)\|^2 + 8 \left(\frac{t+1}{\tau} \right)^2 \mathbb{E} \|\Lambda_i^r - \bar{\Lambda}^r\|^2 + 16(t+1)\eta^2 \frac{\sigma^2}{b}, \quad (24)$$

where we use Assumption 4.1. Next we substitute (24) into (19) to get

$$\begin{aligned}
& \mathbb{E}[\|z_{i,t+1}^r - \mathcal{P}_{\mathcal{M}}(x^r)\|^2] \\
& \leq 16(t+1)\eta^2 L^2 \sum_{\ell=0}^t \mathbb{E}\|z_{i,\ell}^r - \mathcal{P}_{\mathcal{M}}(x^r)\|^2 \\
& \quad + \underbrace{2M^2\tau^2\eta^2\|\text{grad}f(\mathcal{P}_{\mathcal{M}}(x^r))\|^2 + 8\mathbb{E}\|\Lambda_i^r - \bar{\Lambda}^r\|^2 + 16\tau\eta^2\frac{\sigma^2}{b}}_{:=A^r}.
\end{aligned} \tag{25}$$

The following proof is similar to that in [23]. We define A^r as the sum of the last three terms on the right hand of (25) and $S_{i,t}^r := \sum_{\ell=0}^t \mathbb{E}\|z_{i,\ell}^r - \mathcal{P}_{\mathcal{M}}(x^r)\|^2$. By $\mathbb{E}[\|z_{i,t+1}^r - \mathcal{P}_{\mathcal{M}}(x^r)\|^2] = S_{i,t+1}^r - S_{i,t}^r$ and (25), we have

$$S_{i,t+1}^r \leq (1 + 1/(16\tau)) S_{i,t}^r + A^r, \tag{26}$$

where the inequality is from $\tilde{\eta} \leq \eta_g/(16L)$ and thus $16(t+1)\eta^2 L^2 \leq 1/(16\tau)$. With (26), we get

$$S_{i,\tau-1}^r \leq A^r \sum_{\ell=0}^{\tau-2} (1 + 1/(16\tau))^\ell \leq 1.1\tau A^r, \tag{27}$$

where we use $\sum_{\ell=0}^{\tau-2} (1 + 1/(16\tau))^\ell \leq \sum_{\ell=0}^{\tau-2} \exp(\ell/(16\tau)) \leq \sum_{\ell=0}^{\tau-2} \exp(1/16) \leq 1.1\tau$. Summing (27) over all the clients i , we get

$$\begin{aligned}
& \mathbb{E}\left[\sum_{i=1}^n \sum_{t=0}^{\tau-1} \|z_{i,t}^r - \mathcal{P}_{\mathcal{M}}(x^r)\|^2\right] \\
& \leq 3nM^2\tau^3\eta^2\|\text{grad}f(\mathcal{P}_{\mathcal{M}}(x^r))\|^2 + 9\tau\mathbb{E}\|\Lambda^r - \bar{\Lambda}^r\|^2 + 18n\tau^2\eta^2\frac{\sigma^2}{b}
\end{aligned} \tag{28}$$

Now we are ready to bound $\frac{1}{n}\mathbb{E}\|\Lambda^{r+1} - \bar{\Lambda}^{r+1}\|^2$. By the definition of Λ^{r+1} and $\bar{\Lambda}^{r+1}$ we have

$$\begin{aligned}
& \mathbb{E}\|\Lambda^{r+1} - \bar{\Lambda}^{r+1}\|^2 \\
& = \eta^2\mathbb{E}\left\|\tau\text{grad}f(\mathcal{P}_{\mathcal{M}}(\mathbf{x}^{r+1})) - \sum_{t=0}^{\tau-1} \text{grad}f(\mathbf{z}_t^r; \mathcal{B}_t^r) - \tau\overline{\text{grad}f}(\mathcal{P}_{\mathcal{M}}(\mathbf{x}^{r+1})) + \sum_{t=0}^{\tau-1} \overline{\text{grad}f}(\mathbf{z}_t^r; \mathcal{B}_t^r)\right\|^2 \\
& \leq \eta^2\mathbb{E}\left\|\tau\text{grad}f(\mathcal{P}_{\mathcal{M}}(\mathbf{x}^{r+1})) - \sum_{t=0}^{\tau-1} \text{grad}f(\mathbf{z}_t^r; \mathcal{B}_t^r)\right\|^2 \\
& = \eta^2\mathbb{E}\left\|\tau\text{grad}f(\mathcal{P}_{\mathcal{M}}(\mathbf{x}^{r+1})) - \tau\text{grad}f(\mathcal{P}_{\mathcal{M}}(\mathbf{x}^r)) + \tau\text{grad}f(\mathcal{P}_{\mathcal{M}}(\mathbf{x}^r))\right. \\
& \quad \left. - \sum_{t=0}^{\tau-1} \text{grad}f(\mathbf{z}_t^r) + \sum_{t=0}^{\tau-1} \text{grad}f(\mathbf{z}_t^r) - \sum_{t=0}^{\tau-1} \text{grad}f(\mathbf{z}_t^r; \mathcal{B}_t^r)\right\|^2 \\
& \leq 2\eta^2\tau^2 L^2 n\mathbb{E}\|\mathcal{P}_{\mathcal{M}}(\mathbf{x}^{r+1}) - \mathcal{P}_{\mathcal{M}}(\mathbf{x}^r)\|^2 + 4\eta^2\tau L^2 \sum_{i=1}^n \sum_{t=0}^{\tau-1} \mathbb{E}\|z_{i,t}^r - \mathcal{P}_{\mathcal{M}}(x^r)\|^2 + 4\eta^2\tau n\frac{\sigma^2}{b}.
\end{aligned} \tag{29}$$

Here, the first inequality is due to $\|\Lambda^{r+1} - \bar{\Lambda}^{r+1}\|^2 \leq \|\Lambda^{r+1}\|^2$, the last inequality is due to $\|a + b\|^2 \leq 2\|a\|^2 + 2\|b\|^2$, Assumption 4.1, and following similar derivations as in (23).

By substituting (28) into (29) and reorganizing the results, we complete the proof of Lemma A.3. \square

A.3 Proof of Theorem 4.3

To bound the first term in the Lyapunov function, we focus on the server-side update. We begin with the following lemma over the manifolds.

Lemma A.4. Given $x \in \mathcal{M}$, $v \in T_x \mathcal{M}$, $\eta > 0$, $x - \eta v \in \bar{U}_{\mathcal{M}}(\gamma)$, and $x^+ = \mathcal{P}_{\mathcal{M}}(x - \eta v)$, it holds that

$$\begin{aligned} f(x^+) &\leq f(z) + \langle \text{grad} f(x) - v, x^+ - z \rangle \\ &\quad - \frac{1}{2\eta} (\|x^+ - x\|^2 - \|z - x\|^2) - \left(\frac{1}{2\eta} - \frac{3\|v\|}{4\gamma} \right) \|z - x^+\|^2 \\ &\quad + \frac{L}{2} \|x^+ - x\|^2 + \frac{L}{2} \|z - x\|^2, \forall z \in \mathcal{M}. \end{aligned} \quad (30)$$

Proof. For any μ -strongly convex function h , we have for any $y, z \in \mathcal{M}$

$$\begin{aligned} h(z) &\geq h(y) + \langle \nabla h(y), z - y \rangle + \frac{\mu}{2} \|z - y\|^2 \\ &= h(y) + \langle \text{grad} h(y) + \nabla h(y) - \text{grad} h(y), z - y \rangle + \frac{\mu}{2} \|z - y\|^2 \\ &\geq h(y) + \langle \text{grad} h(y), z - y \rangle + \left(\frac{\mu}{2} - \frac{\|\nabla h(y)\|}{4\gamma} \right) \|z - y\|^2, \end{aligned} \quad (31)$$

where the second inequality is from the normal inequality (4) and $\|\nabla h(y) - \text{grad} h(y)\| \leq \|\nabla h(y)\|$. Setting $h(y) = \frac{1}{2\eta} \|y - (x - \eta v)\|^2$ in (31) with $\mu = 1/\eta$, $y = x^+$, and noting the optimality of x^+ (i.e., $\text{grad} h(x^+) = 0$), we have

$$\begin{aligned} \frac{1}{2\eta} \|z - (x - \eta v)\|^2 &\geq \frac{1}{2\eta} \|x^+ - (x - \eta v)\|^2 + \left(\frac{1}{2\eta} - \frac{\|y - (x - \eta v)\|}{4\eta\gamma} \right) \|z - x^+\|^2 \\ &\geq \frac{1}{2\eta} \|x^+ - (x - \eta v)\|^2 + \left(\frac{1}{2\eta} - \frac{3\|v\|}{4\gamma} \right) \|z - x^+\|^2, \end{aligned}$$

where the second inequality is from $x - \eta v \in \bar{U}_{\mathcal{M}}(\gamma)$ and $\|\mathcal{P}_{\mathcal{M}}(x - \eta v) - (x - \eta v)\| \leq \|\mathcal{P}_{\mathcal{M}}(x - \eta v) - x\| + \eta\|v\| \leq 3\eta\|v\|$. Rearranging the above inequality leads to

$$\langle v, z - x^+ \rangle \geq \frac{1}{2\eta} (\|x^+ - x\|^2 - \|z - x\|^2) + \left(\frac{1}{2\eta} - \frac{3\|v\|}{4\gamma} \right) \|z - x^+\|^2. \quad (32)$$

It follows from the L -smoothness of f that

$$\begin{aligned} f(x^+) &\leq f(x) + \langle \text{grad} f(x), x^+ - x \rangle + \frac{L}{2} \|x^+ - x\|^2 \\ &\leq f(z) + \langle \text{grad} f(x), x^+ - z \rangle + \frac{L}{2} \|z - x\|^2 + \frac{L}{2} \|x^+ - x\|^2, \end{aligned}$$

where we use $f(x) + \langle \text{grad} f(x), z - x \rangle - \frac{L}{2} \|z - x\|^2 \leq f(z)$ in the last inequality. Combining the above inequality and (32) gives (30). \square

In the following, we use Lemma A.4 to (7) and (6), respectively. First, to apply Lemma A.4 to (7), we substitute $x^+ = \tilde{x}^{r+1}$, $z = \mathcal{P}_{\mathcal{M}}(x^r)$, $x = \mathcal{P}_{\mathcal{M}}(x^r)$, and $v = \text{grad} f(\mathcal{P}_{\mathcal{M}}(x^r))$ and get

$$\mathbb{E} [f(\tilde{x}^{r+1})] \leq \mathbb{E} \left[f(\mathcal{P}_{\mathcal{M}}(x^r)) + \left(\frac{L}{2} - \frac{1}{2\tilde{\eta}} \right) \|\tilde{x}^{r+1} - \mathcal{P}_{\mathcal{M}}(x^r)\|^2 - \frac{1 - \tilde{\eta}\rho}{2\tilde{\eta}} \|\tilde{x}^{r+1} - \mathcal{P}_{\mathcal{M}}(x^r)\|^2 \right], \quad (33)$$

where we use $\tilde{\eta} \leq \frac{\gamma}{D_f}$ to guarantee $\tilde{x}^{r+1} \in \bar{U}_{\mathcal{M}}(\gamma)$ and $\rho := \frac{3D_f}{2\gamma}$.

Next, to use Lemma A.4 to (6), we set $x^+ = \mathcal{P}_{\mathcal{M}}(x^{r+1})$, $x = \mathcal{P}_{\mathcal{M}}(x^r)$, $z = \tilde{x}^{r+1}$, and $v = v^r$ and get

$$\begin{aligned} &\mathbb{E} [f(\mathcal{P}_{\mathcal{M}}(x^{r+1}))] \\ &\leq \mathbb{E} \left[f(\tilde{x}^{r+1}) + \langle \text{grad} f(\mathcal{P}_{\mathcal{M}}(x^r)) - v^r, \mathcal{P}_{\mathcal{M}}(x^{r+1}) - \tilde{x}^{r+1} \rangle \right. \\ &\quad \left. - \frac{1}{2\tilde{\eta}} (\|\mathcal{P}_{\mathcal{M}}(x^{r+1}) - \mathcal{P}_{\mathcal{M}}(x^r)\|^2 - \|\tilde{x}^{r+1} - \mathcal{P}_{\mathcal{M}}(x^r)\|^2) - \frac{1 - \tilde{\eta}\rho}{2\tilde{\eta}} \|\tilde{x}^{r+1} - \mathcal{P}_{\mathcal{M}}(x^{r+1})\|^2 \right] \end{aligned} \quad (34)$$

$$\begin{aligned}
& + \frac{L}{2} \|\mathcal{P}_{\mathcal{M}}(x^{r+1}) - \mathcal{P}_{\mathcal{M}}(x^r)\|^2 + \frac{L}{2} \|\tilde{x}^{r+1} - \mathcal{P}_{\mathcal{M}}(x^r)\|^2 \\
= & \mathbb{E} \left[f(\tilde{x}^{r+1}) + \langle \text{grad}f(\mathcal{P}_{\mathcal{M}}(x^r)) - v^r, \mathcal{P}_{\mathcal{M}}(x^{r+1}) - \tilde{x}^{r+1} \rangle + \left(\frac{L}{2} - \frac{1}{2\tilde{\eta}} \right) \|\mathcal{P}_{\mathcal{M}}(x^{r+1}) - \mathcal{P}_{\mathcal{M}}(x^r)\|^2 \right. \\
& \left. + \left(\frac{L}{2} + \frac{1}{2\tilde{\eta}} \right) \|\tilde{x}^{r+1} - \mathcal{P}_{\mathcal{M}}(x^r)\|^2 - \frac{1-\tilde{\eta}\rho}{2\tilde{\eta}} \|\mathcal{P}_{\mathcal{M}}(x^{r+1}) - \tilde{x}^{r+1}\|^2 \right],
\end{aligned}$$

where we use $\tilde{\eta} \leq \frac{\gamma\eta_a}{2D_f}$ to guarantee $\mathcal{P}_{\mathcal{M}}(x^{r+1}) \in \bar{U}_{\mathcal{M}}(\gamma)$.

Combining (33) and (34) yields

$$\begin{aligned}
& \mathbb{E} [f(\mathcal{P}_{\mathcal{M}}(x^{r+1}))] \tag{35} \\
\leq & \mathbb{E} \left[f(\mathcal{P}_{\mathcal{M}}(x^r)) + \left(L - \frac{1}{2\tilde{\eta}} + \frac{\rho}{2} \right) \|\tilde{x}^{r+1} - \mathcal{P}_{\mathcal{M}}(x^r)\|^2 + \left(\frac{L}{2} - \frac{1}{2\tilde{\eta}} \right) \|\mathcal{P}_{\mathcal{M}}(x^{r+1}) - \mathcal{P}_{\mathcal{M}}(x^r)\|^2 \right. \\
& \left. - \underbrace{\frac{1-\tilde{\eta}\rho}{2\tilde{\eta}} \|\mathcal{P}_{\mathcal{M}}(x^{r+1}) - \tilde{x}^{r+1}\|^2}_{\text{(IV)}} + \underbrace{\langle \mathcal{P}_{\mathcal{M}}(x^{r+1}) - \tilde{x}^{r+1}, \text{grad}f(\mathcal{P}_{\mathcal{M}}(x^r)) - v^r \rangle}_{\text{(V)}} \right].
\end{aligned}$$

According to $\|a + b\|^2 \leq \frac{1}{2\tilde{\eta}}\|a\|^2 + \frac{\tilde{\eta}}{2}\|b\|^2$, we have

$$\begin{aligned}
& \text{(IV)} + \text{(V)} \tag{36} \\
\leq & \text{(IV)} + \frac{1-\tilde{\eta}\rho}{2\tilde{\eta}} \|\mathcal{P}_{\mathcal{M}}(x^{r+1}) - \tilde{x}^{r+1}\|^2 + \frac{\tilde{\eta}}{2(1-\tilde{\eta}\rho)} \|\text{grad}f(\mathcal{P}_{\mathcal{M}}(x^r)) - v^r\|^2 \\
= & \frac{\tilde{\eta}}{2(1-\tilde{\eta}\rho)} \|\text{grad}f(\mathcal{P}_{\mathcal{M}}(x^r)) - v^r\|^2.
\end{aligned}$$

To bound the above inequality, following similar derivations as in (23) we obtain

$$\begin{aligned}
& \mathbb{E} \|v^r - \text{grad}f(\mathcal{P}_{\mathcal{M}}(x^r))\|^2 \\
= & \mathbb{E} \left\| \frac{1}{n\tau} \sum_{i=1}^n \sum_{t=0}^{\tau-1} \left(\text{grad}f_i(z_{i,t}^r; \mathcal{B}_{i,t}^r) - \text{grad}f_i(z_{i,t}^r) + \text{grad}f_i(z_{i,t}^r) - \text{grad}f_i(\mathcal{P}_{\mathcal{M}}(x^r)) \right) \right\|^2 \tag{37} \\
\leq & 2L^2 \frac{1}{n\tau} \sum_{i=1}^n \sum_{t=0}^{\tau-1} \mathbb{E} \|z_{i,t}^r - \mathcal{P}_{\mathcal{M}}(x^r)\|^2 + \frac{2}{\tau n} \frac{\sigma^2}{b}.
\end{aligned}$$

Substituting (36) and (37) into (35), we have

$$\begin{aligned}
& \mathbb{E}[f(\mathcal{P}_{\mathcal{M}}(x^{r+1}))] \tag{38} \\
\leq & \mathbb{E} \left[f(\mathcal{P}_{\mathcal{M}}(x^r)) + \left(L - \frac{1}{2\tilde{\eta}} + \frac{\rho}{2} \right) \|\tilde{x}^{r+1} - \mathcal{P}_{\mathcal{M}}(x^r)\|^2 + \left(\frac{L}{2} - \frac{1}{2\tilde{\eta}} \right) \|\mathcal{P}_{\mathcal{M}}(x^{r+1}) - \mathcal{P}_{\mathcal{M}}(x^r)\|^2 \right. \\
& \left. + \frac{\tilde{\eta}}{2(1-\tilde{\eta}\rho)} \left(\frac{2L^2}{n\tau} \sum_{i=1}^n \sum_{t=0}^{\tau-1} \|z_{i,t}^r - \mathcal{P}_{\mathcal{M}}(x^r)\|^2 + \frac{2}{\tau n} \frac{\sigma^2}{b} \right) \right].
\end{aligned}$$

The final term is the drift-error that can be bounded in (28). Thus, (38) becomes

$$\begin{aligned}
& \mathbb{E}[f(\mathcal{P}_{\mathcal{M}}(x^{r+1}))] \tag{39} \\
\leq & \mathbb{E} \left[f(\mathcal{P}_{\mathcal{M}}(x^r)) + \left(L - \frac{1}{2\tilde{\eta}} + \frac{\rho}{2} \right) \|\tilde{x}^{r+1} - \mathcal{P}_{\mathcal{M}}(x^r)\|^2 + \left(\frac{L}{2} - \frac{1}{2\tilde{\eta}} \right) \|\mathcal{P}_{\mathcal{M}}(x^{r+1}) - \mathcal{P}_{\mathcal{M}}(x^r)\|^2 \right. \\
& \left. + \frac{\tilde{\eta}}{2(1-\tilde{\eta}\rho)} \frac{2L^2}{n\tau} \left(12nM^2\tau^3\eta^2 \|\mathcal{G}_{\tilde{\eta}}(\mathcal{P}_{\mathcal{M}}(x^r))\|^2 + 9\tau\mathbb{E}\|\mathbf{\Lambda}^r - \bar{\mathbf{\Lambda}}^r\|^2 + 18n\tau^2\eta^2\frac{\sigma^2}{b} \right) + \frac{\tilde{\eta}}{2(1-\tilde{\eta}\rho)} \frac{2}{\tau n} \frac{\sigma^2}{b} \right],
\end{aligned}$$

where we use $\|\text{grad}f(\mathcal{P}_{\mathcal{M}}(x^r))\| \leq 2\|\mathcal{G}_{\tilde{\eta}}(\mathcal{P}_{\mathcal{M}}(x^r))\|$ from Lemma (A.2). By substituting $\tilde{\eta} \leq \frac{1}{4\rho}$ as $\tilde{\eta} \leq \frac{\gamma}{6D_f}$, we have $\frac{\tilde{\eta}}{2(1-\tilde{\eta}\rho)} \leq \tilde{\eta}$. Combining the recursions given by Lemma A.3 and (39), we have for the Lyapunov function that

$$\begin{aligned} & \mathbb{E} \left[(f(\mathcal{P}_{\mathcal{M}}(x^{r+1})) - f^*) + \frac{1}{\tilde{\eta}n} \|\mathbf{\Lambda}^{r+1} - \overline{\mathbf{\Lambda}}^{r+1}\|^2 \right] \\ & \leq \mathbb{E} \left[(f(\mathcal{P}_{\mathcal{M}}(x^r)) - f^*) + \frac{1}{\tilde{\eta}n} \|\mathbf{\Lambda}^r - \overline{\mathbf{\Lambda}}^r\|^2 - \frac{\tilde{\eta}}{8} \|\mathcal{G}(\mathcal{P}_{\mathcal{M}}(x^r))\|^2 \right] + \frac{8\tilde{\eta}}{n\tau} \frac{\sigma^2}{b}, \end{aligned} \quad (40)$$

where we substitute conditions (11) on the step sizes and omit straightforward algebraic calculations. Substituting the definition of the Lyapunov function Ω^r and repeating the above inequality, we complete the proof of Theorem 4.3.

A.4 Additional results for numerical experiments

A.4.1 kPCA

The settings for Mnist Dataset. The Mnist dataset consists of 60,000 handwritten digit images ranging from 0 to 9, each with dimensions of 28×28 . We reshape these images into a data matrix $A \in \mathbb{R}^{60000 \times 784}$. To construct the heterogeneous A_i , we sort the rows in increasing order of their associated digits and then split every $60000/n$ rows, with $n = 10$ as the number of clients, among each client. In our setup, $d = 784$, $p = 6000$, and $k = 2$.

For kPCA problem with Mnist dataset, the comparison on $f(x^r) - f^*$ is shown in Fig. 5.

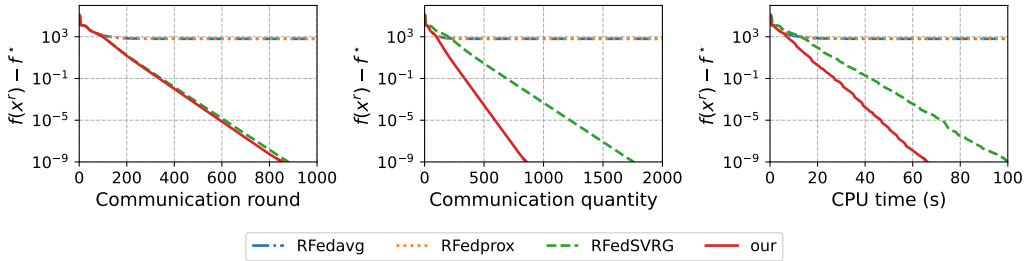


Figure 5: kPCA problem with Mnist dataset: Comparison on $f(x^r) - f^*$.

Synthetic Dataset. We also solve kPCA with synthetic datasets on larger networks with $n = 30$. We generate each entry of A_i from Gaussian distribution $\mathcal{N}(0, \frac{2i}{n})$ such that A_i are heterogeneous among clients. We set $(d, k) = (20, 5)$ and $p = 15$. We use the local full gradient ∇f_i to remove the influence of stochastic Riemannian gradient noise.

In the first set of experiments, we compare with existing algorithms, including RFedavg, RFedprox, and RFedSVRG. For all algorithms, we set the number of local steps as $\tau = 5$ and the step size as $\eta = 4e-3$. For our algorithm, we set $\eta_g = 1$. The experimental results are shown in Fig. 6. The y -axis represents $\|\text{grad}f(x^r)\|$ and $(f(x^r) - f^*)$ respectively, while the x -axis represents the number of communication rounds, communication quantity, and CPU time, respectively. It can be observed that RFedavg and RFedprox face the issue of client drift, hence they do not converge accurately. Both FedSVRG and our algorithm can overcome the client drift issue, but our algorithm is slightly faster in terms of communication rounds and is much faster in terms of both communication quantity and running time.

In the second set of experiments, we test the impact of the number of local updates τ . For all the algorithms, we set $R = 4000$, the step size $\eta = 0.7e-3$, and $\tau \in \{10, 15, 20\}$. For our algorithm, we set $\eta_g = 1$. The results are shown in Fig. 7, with the y -axis representing $\|\text{grad}f(x^r)\|$ and x -axis representing the communication quantity. When τ increases, the convergence becomes faster. For all values of τ , our algorithm achieves high accuracy and requires less time.

A.4.2 Low-rank matrix completion

For numerical tests, we consider random generated A . To be specific, we first generate two random matrices $\hat{L} \in \mathbb{R}^{d \times k}$ and $\hat{R} \in \mathbb{R}^{k \times T}$, where each entry obeys the standard Gaussian distribution.

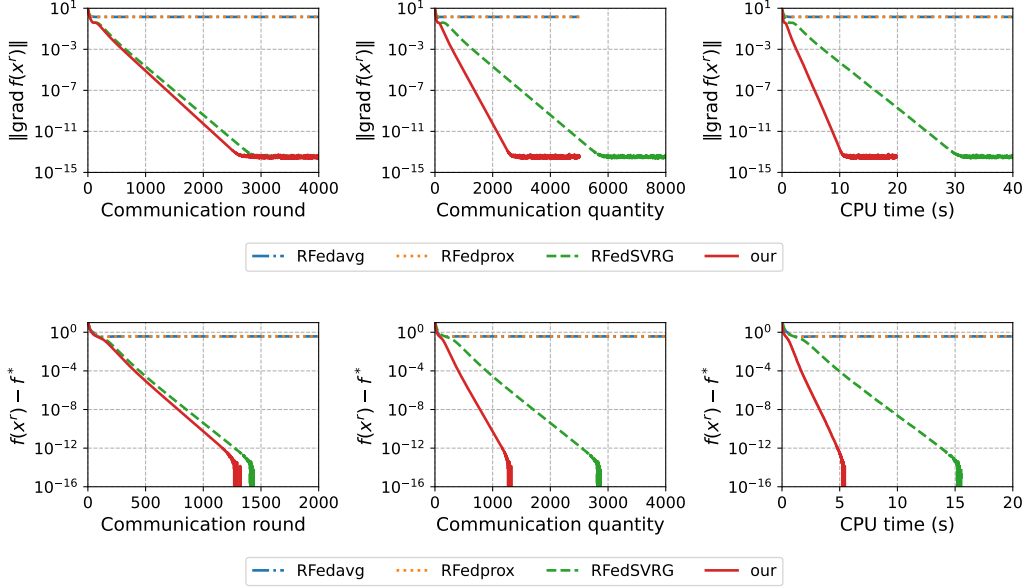


Figure 6: kPCA with synthetic dataset: Comparison on $\|\text{grad} f(x^r)\|$ and $f(x^r) - f^*$.

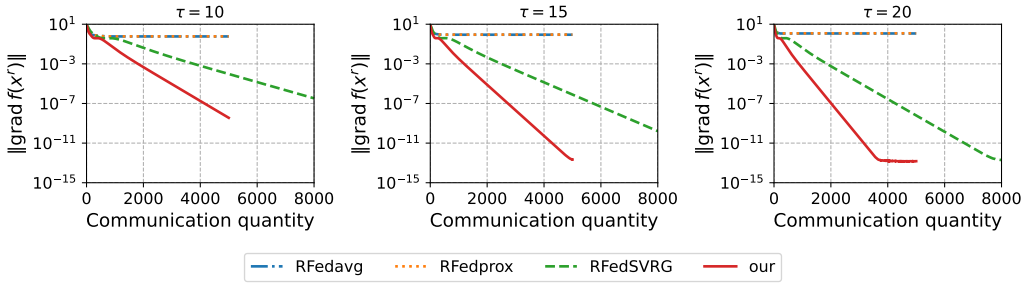


Figure 7: kPCA with synthetic dataset: The impacts of τ .

For the indices set Ω , we generate a random matrix B with each entry following from the uniform distribution, then set $\Omega_{ij} = 1$ if $B_{ij} \leq \nu$ and 0 otherwise. The parameter ν is set to $10k(d + T - k)/(dT)$.

As shown in Fig. 8, our algorithm is faster than existing algorithms in terms of communication quantity and running time.

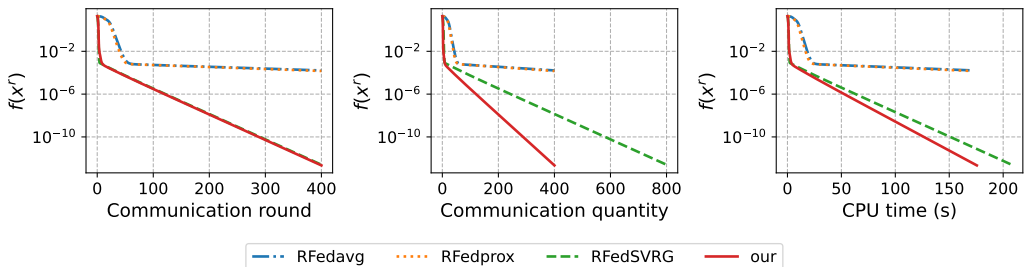


Figure 8: LRMC: Comparison on $f(x^r)$.

We also show the impacts of τ . As shown in Fig. 9, larger τ yields less communication quantity to achieve the same accuracy.

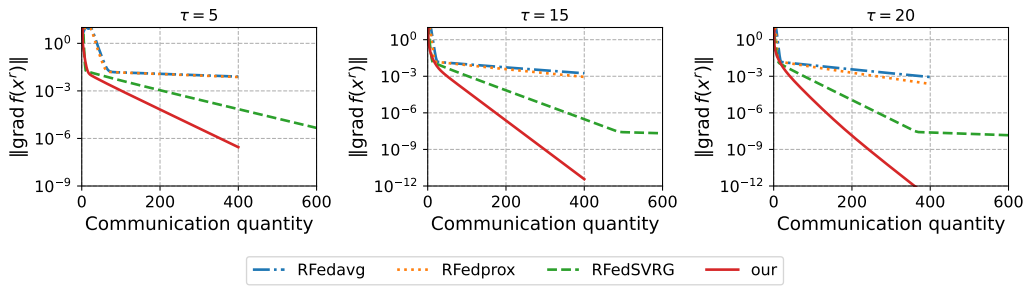


Figure 9: LRMC: The impacts of τ .